Wall Conditioning by ECRH and GDC at the Wendelstein 7-X Stellarator

T. Wauters[1], T. Stange[2], H.P. Laqua[2], R. Brakel[2], S. Marsen[2], D. Moseev[2], T. Sunn Pedersen[2], O. Volzke[2], S. Brezinsek[3], A. Dinklage[2] and the W7-X team.

[1]*Laboratory for Plasmaphysics, LPP-ERM/KMS, Brussels, Belgium, TEC Parner*

[2]*Max-Planck-Institute for Plasma Physics, Greifswald, Germany*

[3]*Forschungszentrum Jülich, Jülich, Germany, TEC Parner*

Introduction

Wall conditioning in magnetic controlled fusion devices is a common tool to improve plasma performance and discharge reproducibility [1]. It will be relied upon in the next W7-X operation phases (OP1.2 in 2017-2018 and OP2 starting in 2020) to control the surface state of the plasma-facing components (PFC) with the eventual aim of providing access to continuous discharge operation [2]. The super-conducting stellarator W7-X keeps its magnetic field charged during the experimental days. Therefore conventional wall conditioning by glow discharges cannot be routinely used and alternatively RF-based wall conditioning scenarios are foreseen. The multi-megawatt ECRH system [3], operational during the first operation campaign (OP1.1) of W7-X, is well suited for this purpose, since in a stellarator the confining magnetic field already exists in the vacuum. The confined ECRH plasma could be sufficiently dense and hot to provide good absorption of ECRH power minimizing stray radiation. Conditioning by ICRH discharges will become available in the next operation campaign OP1.2.

This contribution analyses the performance improvement of W7-X plasmas by means of GDC and Electron Cyclotron Wall Conditioning (ECWC) throughout OP1.1. All discharges are performed in limiter configuration on 5 inertially cooled graphite limiters [4]. Vacuum vessel and PFC conditioning of W7-X prior to plasma operation consisted of 1 week of baking at 150°C without any Glow Discharge Conditioning (GDC). As such, many plasma impurities such as oxygen, nitrogen, carbondioxide, water etc. were expected. Overall, the usage of GDC operation between operational days was limited throughout the campaign to avoid copper sputtering and migration as max. 20% of the copper cooling structures were covered by carbon protection tiles. A total of 10.9 h of He-GDC was performed. The experimental arrangement for GDC on W7-X involves 10 graphite DC anodes at 250 to 500V, positioned within the vacuum vessel (one per half module) [5].

Normalized outgassing

Within the context of this paper, the W7-X plasma performance is evaluated by following parameters: (i) plasma discharge duration, (ii) injected energy and (iii) outgassing pressure peak at the end of the discharge (as a measure of the release rate of gas from the PFC's). Figure 1 shows the evolution of the outgassing pressure peak normalized to the injected energy as a function of the cumulated discharge duration of W7-X ERCH plasmas in the initial He-phase of the campaign. At the start of the campaign, the normalized outgassing was of order $5 \cdot 10^{-6}$ mbar/kJ. On average 10 kJ of ECRH energy was injected in a 10 ms plasma, before the discharge terminates by a radiative collapse producing an outgassing peak of $\sim 5 \cdot 10^{-5}$ mbar. Mass spectrometry showed a strong release of CO as well as H_2. Outgassing of H_2O and hydrocarbons occurred at lower rates. No ion saturation current was observed on the limiter Langmuir probes in the first W7-X discharges, and the temperature rose less than 2 °C. The gas release is therefore thought to be triggered by photon stimulated desorption and impact of reactive low energy Franck-Condon H atoms (~ 2.2 eV) stemming from electron impact dissociation of wall-released H_2 molecules. Within 30 to 45 s of cumulated discharge time, the normalized outgassing improves to $3 \cdot 10^{-8}$ mbar/kJ, allowing sustaining 0.1 s pulses while injecting ~2.5 MW, producing an outgassing peak of $\sim 1 \cdot 10^{-5}$ mbar.

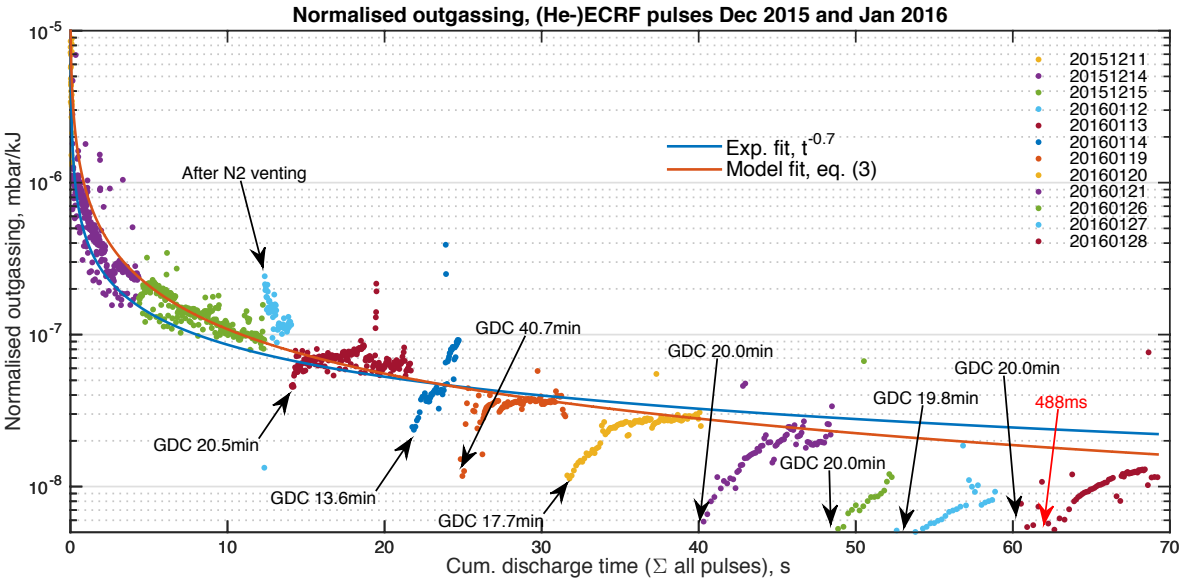

Figure 1: Normalised outgassing: experimental data (dots), typical experimental typical $t^{-0.7}$ (blue line) and fit by eq. (3) (red line), fitting parameters are discussed in the text. The discontinuities in the outgassing trend are result of GDC operation, indicated by arrows.

It is clearly seen that short He-GDC leads to He-ion-induced desorption of hydrogen and intrinsic impurities, resulting in unsaturated wall components characterized by a temporary improvement of the outgassing, and, as a consequence, of the discharge performance. Similar observations in tokamaks with carbon PFCs have been seen in TEXTOR [6] and DIII-D [7]. Wall conditioning by GDC provided access to 0.5 s pulses and 2 MJ of injected power per pulse towards the end of the He-phase, successfully concluding the first half of the very first operation campaign of W7-X.

Release models

The normalized outgassing trend corresponds to the typical $t^{-0.7}$dependence, observed also on JET (C & ILW [8]), TORE SUPRA [9] and other devices [10]. The power law originates from processes such as included in Andrew's model [11], which derives from trapping site concentrations, detrapping, retrapping and recombination to molecule. We repeat below the main equations of the model, eq. (1) and eq. (2) [11]:

$$\frac{\partial c_t}{\partial t} = -K_{ts}c_t + K_{st}c_s\left(1-\frac{c_t}{c_0}\right) \quad (1), \qquad \frac{\partial (c_s+c_t)}{\partial t} = -K_r c_s^2 \quad (2), \qquad \frac{dc}{dt} \approx -K\frac{c^2}{\left(1-c/c_0\right)} \quad (3)$$

They essentially represent the exchange of atoms (H) between two states 't' and 's'. K_{ts} and K_{st} are the rate constants associated with detrapping from 't' into 's' and retrapping respectively. The possible concentration c in state 't' is finite and limited by c_0. The release rate of gas is $K_r c_s^2$ and occurs from state 's' with (recombination) rate K_r. When $c = c_t + c_s \approx c_t$, the outgassing rate is approximated by eq. (3) with $K = K_r(K_{ts}/K_{st})^2$. [11]

The outgassing rate following from eq. (3) is plotted in red in Figure 1 with $Kc_0 = 1{\cdot}10^{-2}$ and $c(t=0) = 0.95c_0$.

Further exploring the outgassing rate by eq. (1) and (2) illustrates the distinct effects of GDC and ECRH discharges. The result is shown on Figure 2. The blue dots represent the experimental normalized outgassing data for every ECRH pulse in the OP1.1 campaign (discharge gas includes He, H_2 and Ar), while the outgassing rate following from eq. (3) is plotted again in red using the same fitting parameters as above. It is clear that He and H_2-ECRH discharges follow the same trend, and as such outgassing continues to play a major role. Towards the end of the campaign, the normalized outgassing decreased further to an average value of $3{\cdot}10^{-9}$ mbar/kJ, whereas after GDC values below $1{\cdot}10^{-9}$ mbar/kJ allowed to sustain 6 sec pulses at low ECRF power, staying within the (in OP1.1) maximum allowed 4 MJ [4] of energy.

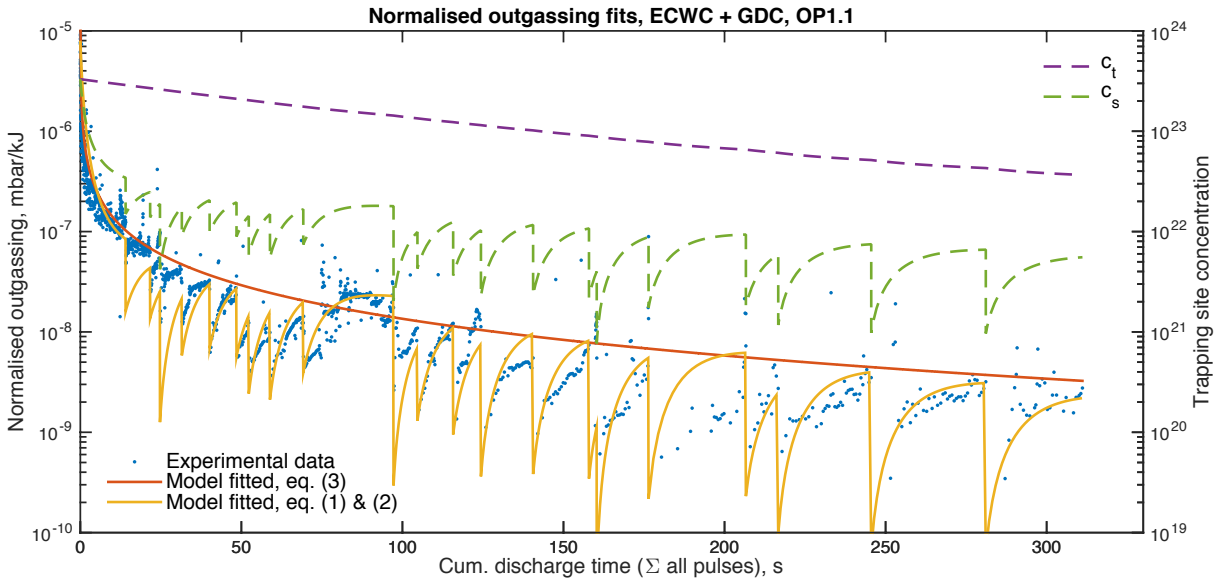

Figure 2: Left axis: Normalised outgassing: experimental data (blue dots), fit using eq. (3) (red line) and fit using eq. (1) and (2) including the conditioning contribution by GDC (yellow line). Right axis: Trapping site concentrations in particle reservoirs 't' (purple) and 's' (green) following from latter (yellow) fit

The outgassing rate modeled by eq. (1) and (2) is plotted in yellow. The curve includes the discontinuities that are produced by short (5 to 40 mins) He-GDC. The experimentally observed normalized outgassing rate could be reproduced by making following assumptions: The decrease in time of $c_t + c_s$ defines the release rate of molecules from the walls. The volume of the W7-X vacuum vessel (~ $3{\cdot}10^5$ l at 300 K) relates the number of molecules to pressure. Considering an averaged ECRH power of 3 MW in OP1.1 retrieves the normalized outgassing rate. The rate constants during H_2 and He ECRH plasmas are fixed at $K_r = 3{\cdot}10^{-24}$, $K_{ts} = 0.01$ and $K_{st} = 0.05$ (resulting in $Kc_0 = 4{\cdot}10^{-2}\mathrm{s}^{-1}$). The initial concentration for sites 't' and 's' are set $c_t(t=0) = c_s(t=0) = 3.3{\cdot}10^{23}$. He-GDC removes atoms from state 's' only, setting $K_{ts} = K_{st} = 0$ during the GDC. The removed amount of atoms by a GDC procedure is estimated as $\int I_{GDC} Y_{GDC} c_s \, \mathrm{d}t$, with physical He ion sputtering yield $Y_{GDC} = 3{\cdot}10^{-5}\mathrm{C}^{-1}$ (e.g. [12]) and glow current I_{GDC}, measured at the DC generators.

Conditioning contributions of ECRH and GDC

The time evolution of the trapping site concentration modeled by eq. (1) and (2) are shown on the right axis of Figure 2 in purple (c_t) and green (c_s) respectively. It is concluded from these curves that hydrogen/impurity removal from c_t by ECRH discharges is a slow (factor 10 in 311 s) but necessary process. Depleting c_s by He-GDC has little effect on c_t in the subsequent ECRH discharges, but it results in a temporary improvement of the normalized outgassing and therefor also of the achievable injected energy levels. Long pulse operation on W7-X may require a strongly depleted c_t as nearly all ECRH discharges ended with a radiative collapse due to too strong outgassing by the PFC's.

Throughout the campaign $c_t + c_s$ was reduced by $6.2{\cdot}10^{23}$ atoms, corresponding e.g. to $3.1{\cdot}10^{23}$ H_2 molecules

Gas balance

Figure 3 presents the gas balance per experiment (sequence of launched ECRH pulses). The injected amount of gas (blue) is obtained by integrating the calibrated gas flows corrected for the gas type (He, H_2 or Ar). The pumped amount of gas (red) in each experiment is obtained by the integral of the neutral pressure time traces including discharge and post-discharge phase, multiplied by the pumping speed. Accounting for the gas composition of the residual gas was not feasible. It is assumed that the majority of the outgassed species consist of H_2 molecules.

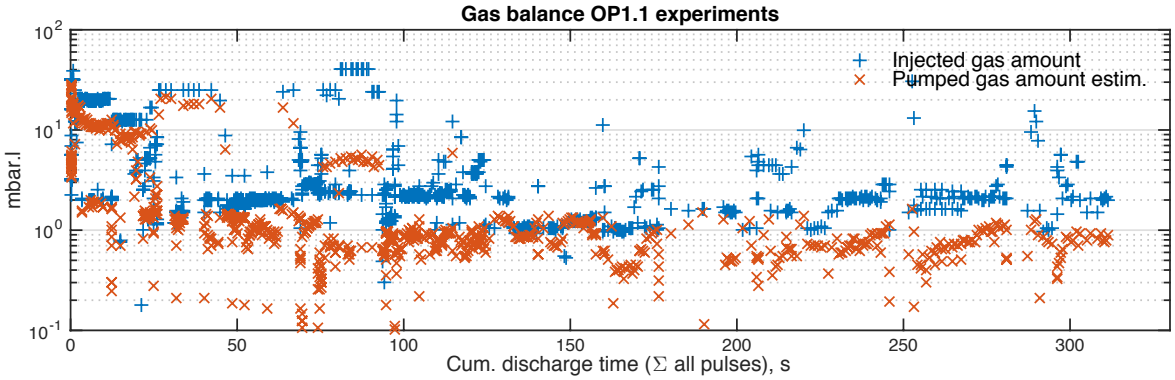

Figure 3: Gas balance per experiment (may include multiple ECRH pulses) as function of cumulated RF discharge time for all OP1.1 experiments. Blue: injected amount (He+H_2+Ar), red pumped amount (assumed H_2 pumping speed).

The balance shows that on average ~5 times more gas is pumped than injected: the total injected amounts 4.9 bar.l, while the pumped amount equals about 22 bar.l when assuming light species such as H_2. The latter corresponds to a net amount of $4.2 \cdot 10^{23}$ molecules, in close agreement with the number obtained in the above analysis. Although recycling is closer to 1 after He-GDC, it seems that there is no significant improvement throughout the campaign.

Conclusion

The OP1.1 limiter ECRF pulses 'suffered' from low plasma purity and density control. Outgassing dominated the fueling of the ECRH discharges throughout OP1.1. The majority of pulses in OP1.1, beit in limiter configuration and with limited pre-conditioning, ended by a radiative collapse. OP1.1. Prior to operation, long GDC in H_2 or D_2 is required to deplete walls from impurities (CO, CO_2 and H_2O). Temporarily depleting the walls from the remaining H is possible by He-GDC, while more than the achieved 311 cumulated discharge seconds of ECRH discharges seem needed for obtaining lastingly low outgassing levels. Obtaining such discharge duration proved to be time consuming as the pulse duration of an (X2-)ERCH discharge is limited by outgassing. ICRH conditioning may overcome this difficulty. ICRF waves couple efficiently to low density, low temperature plasma, even in the presence of impurities, and at full operating field (B = 2.5 T) in W7-X. ICWC might therefore be the method of choice in W7-X for wall conditioning in future operation phases.

This work has been carried out within the framework of the EUROfusion Consortium and has received funding from the Euratom research and training programme 2014-2018 under grant agreement No 633053. The views and opinions expressed herein do not necessarily reflect those of the European Commission.

References

[1] J. Winter, Plasma Phys. Control. Fusion 38 (1996)1503.
[2] R. Wolf and Wendelstein Team, Fusion Eng. Des. 83, 990 (2008).
[3] V. Erckmann et al., Fusion Science Techn. 52, 291 (2007).
[4] T. Sunn Pedersen et al., P4.001, This conference.
[5] A. Spring, Fusion Eng. and Des. 66-68, 371-375 (2003).
[6] J. Winter et al., Journal of Nuclear Materials 93 & 94 (1980) 812-819.
[7] G. L. Jackson, Nuclear Fusion, Vol. 30, No. 11 (1990).
[8] V. Philipps et al., Journal of Nuclear Materials 438 (2013) S1067–S1071.
[9] S. Panayotis et al., Journal of Nuclear Materials 438 (2013) S1059–S1062.
[10] M. Mayer et al., Journal of Nuclear Materials 290-293 (2001) 381-388.
[11] P. Andrew and M. Pick, Journal of Nuclear Materials 220-222 (1995) 601-605.
[12] H. F. Dylla, AIP Conference Proceedings 199, 3 (1990)